



## Get Clarity On Generics

Cost-Effective CT & MRI Contrast Agents

**FRESENIUS  
KABI**

[WATCH VIDEO](#)

# AJNR

## Proton MR Spectroscopy Provides Relevant Prognostic Information in High-Grade Astrocytomas

C. Majós, J. Bruna, M. Julià-Sapé, M. Cos, Á. Camins, M. Gil, J.J. Acebes, C. Aguilera and C. Arús

This information is current as of August 10, 2025.

*AJNR Am J Neuroradiol* 2011, 32 (1) 74-80

doi: <https://doi.org/10.3174/ajnr.A2251>

<http://www.ajnr.org/content/32/1/74>

ORIGINAL  
RESEARCH

C. Majós  
J. Bruna  
M. Julià-Sapé  
M. Cos  
Á. Camins  
M. Gil  
J.J. Acebes  
C. Aguilera  
C. Arús



# Proton MR Spectroscopy Provides Relevant Prognostic Information in High-Grade Astrocytomas

**BACKGROUND AND PURPOSE:** There is a large range of survival times in patients with HGA that can only be partially explained by histologic grade and clinical aspects. This study aims to retrospectively assess the predictive value of single-voxel  $^1\text{H}$ -MRS regarding survival in HGA.

**MATERIALS AND METHODS:** Pretreatment  $^1\text{H}$ -MRS in 187 patients with HGA produced 180 spectra at STE (30 ms) and 182 at LTE (136 ms). Patients were dichotomized into 2 groups according to survival better or worse than the median. The spectra of the 2 groups were compared using the Mann-Whitney  $U$  test. The points on the spectrum with the most significant differences were selected for discriminating patients with good and poor prognosis. Thresholds were defined with ROC curves, and survival was analyzed by using the Kaplan-Meier method and the Cox proportional hazards model.

**RESULTS:** Four points on the spectrum showed the most significant differences: 0.98 and 3.67 ppm at STE; and 0.98 and 1.25 ppm at LTE ( $P$  between  $<.001$  and  $.011$ ). These points were useful for stratifying 2 prognostic groups ( $P$  between  $<.001$  and  $.003$ , Kaplan-Meier). The Cox forward stepwise model selected 3 spectroscopic variables: the intensity values of the points 3.67 ppm at STE (hazard ratio, 2.132; 95% CI, 1.504–3.023), 0.98 ppm at LTE (hazard ratio, 0.499; 95% CI, 0.339–0.736), and 1.25 ppm at LTE (hazard ratio, 0.574; 95% CI, 0.368–0.897).

**CONCLUSIONS:**  $^1\text{H}$ -MRS is of value in predicting the length of survival in patients with HGA and could be used to stratify prognostic groups.

**ABBREVIATIONS:**  $^1\text{H}$ -MRS = proton MR spectroscopy; Cho = choline-containing compounds; CI = confidence interval; DWI = diffusion-weighted imaging; HGA = high-grade astrocytomas; I = intensity; KPS = Karnofsky Performance Status; LTE = long TE; MGMT = O6-methylguanine–DNA methyltransferase; NI = normalized intensity; NS = not significant; PWI = perfusion-weighted imaging; ROC = receiver operating characteristic analysis; SE = spin-echo; STE = short TE; VOI = volume of interest; WHO = World Health Organization

High-grade astrocytomas (WHO class III or IV) are the most common glial tumors. The survival rate for patients with these tumors is poor and ranges between a few days and several years.<sup>1,2</sup> The reasons for this large variability from patient to patient are not fully understood. Treatment with chemotherapy and/or radiation therapy can be offered and has been found to improve overall survival and progression-free survival.<sup>3,4</sup> A precise prognostic assessment of these patients, as well as some predictive evaluation of survival after treatment, would be helpful to decide the indication for intensive

treatments. Histopathologic WHO grade remains the best prognosis factor for these tumors, but this assessment can be inappropriate in some cases because of sampling error,<sup>5</sup> the large range of the WHO classification, interpathologist and intrapathologist variability,<sup>6,7</sup> and the difference in the biology of tumors within the same WHO grade.<sup>8</sup> Other prognostic factors, such as age, extent of surgery, and KPS, have been found to be useful in specifying the prognosis.<sup>9,10</sup>

Functional MR imaging techniques, such as DWI, PWI, and  $^1\text{H}$ -MRS, yield structural and metabolic information that may provide better insight into tumor functionality and improve the prognostic stratification of brain tumors.<sup>11</sup> Recent work has shown the potential of DWI and PWI in discriminating tumors of good and poor prognosis in the brain.<sup>12–14</sup> Oh et al<sup>15</sup> found a significantly shorter median survival time for patients with a large volume of metabolic abnormality, measured by  $^1\text{H}$ -MRS. Additional studies have evaluated some particular resonances of the spectrum and have found them to be useful for predicting patient outcome in gliomas.<sup>16,17</sup> The purpose of our study was to determine which regions of the spectrum, evaluated both at STE and LTE, were the most relevant for predicting survival in HGA and to analyze the potential of  $^1\text{H}$ -MRS for discriminating patients with good and poor prognosis.

## Materials and Methods

### Patients

Prior written informed consent for routine MR imaging studies was obtained from all patients. This retrospective study was approved by

Received April 7, 2010; accepted after revision June 23.

From the Department of Radiology (C.M., M.C., Á.C., C. Aguilera), Institut de Diagnòstic per la Imatge, Centre Bellvitge, Hospital Universitari de Bellvitge, L'Hospitalet de Llobregat, Spain; Department of Neurology (J.B.), Hospital Universitari de Bellvitge, L'Hospitalet de Llobregat, Spain; Centro de Investigación en Red en Bioingeniería (C.M., M.J.-S., J.J.A., C. Aguilera, C. Arús), Biomateriales y Nanomedicina, Cerdanyola del Vallès, Spain; Department de Bioquímica i Biologia Molecular (M.J.-S., C. Arús), Unitat de Bioquímica de Biociències, Universitat Autònoma de Barcelona, Cerdanyola del Vallès, Spain; Department of Medical Oncology (M.G.), Institut Català d'Oncologia, Hospital Universitari de Bellvitge, L'Hospitalet de Llobregat, Spain; and Department of Neurosurgery (J.J.A.), Hospital Universitari de Bellvitge, L'Hospitalet de Llobregat, Spain.

This work was supported in part by PHENOIMA (Ministerio de Educación y Ciencia SAF 2008–03323); CIBER-BBN, which is an initiative funded by the VI National R&D&I Plan 2008–2011; Iniciativa Ingenio 2010, Consolider Program, CIBER Actions; and the Instituto de Salud Carlos III with assistance from the European Regional Development Fund, Spain.

Please address correspondence to Carles Majós, MD, Institut de Diagnòstic per la Imatge, Centre Bellvitge, Hospital Universitari de Bellvitge, Autovia de Castelldefels km 2.7, 08907 L'Hospitalet de Llobregat, Spain; e-mail: cmajos@bellvitgehospital.cat



Indicates open access to non-subscribers at [www.ajnr.org](http://www.ajnr.org)

DOI 10.3174/ajnr.A2251

the institutional review board of our hospital with a waiver of specific informed patient consent. We retrospectively selected all patients who had been studied at our hospital with <sup>1</sup>H-MRS on the diagnostic pretreatment examination and who met the following inclusion criteria: 1) pathologically confirmed high-grade astrocytoma (WHO class III or IV); 2) absence of oncologic treatment, including surgical biopsy, before <sup>1</sup>H-MRS; 3) spectra of good quality at a visual inspection; and 4) availability of all the clinical data required for the study (age, sex, WHO histology grade, extent of surgery, KPS, treatment administered, and overall survival). A spectrum was considered to be of poor quality when large peak linewidth, poor signal intensity-to-noise ratio, or obvious artifacts precluded precise quantification of some areas of the spectrum. Death related to surgery was considered an exclusion criterion.

A total of 291 consecutive patients with HGA (criterion 1) were studied with <sup>1</sup>H-MRS at our hospital between August 1997 and August 2009. Of them, 21 patients were excluded because of prior oncologic treatment (criterion 2). In 43 patients, spectra obtained at both TEs were considered to be of poor quality and the patients were excluded (criterion 3). Seven additional spectra at STE and 5 at LTE were excluded, but patients were retained in the study because the spectrum at 1 TE (short or long) was of satisfactory quality in the assessment. Twenty-five patients could not be included because they were lost to follow-up and some clinical data could not be obtained (criterion 4). Finally, 15 patients were excluded because death was related to postsurgical complications. As a consequence, the definitive dataset of the study included 180 spectra at STE and 182 at LTE, pertaining to 187 patients.

Patient medical records were reviewed by 2 authors (C.M. and J.B.), and data about age, sex, WHO histology grade (III or IV), extent of surgery (biopsy, partial resection, or complete resection), KPS after surgery, treatment administered (conservative support, radiation therapy alone, or chemoradiotherapy), and overall survival were collected. In all cases, patient treatment after histologic diagnosis, as well as in tumor recurrence, was decided in the multidisciplinary neuro-oncology unit of our hospital on the basis of standard management. Our protocol for the treatment of malignant astrocytomas consists of maximal surgical debulking to the greatest possible extent followed by standard focal radiation therapy (30 × 2 Gy) plus concomitant (75 mg per square meter of body surface area per day, 7 days per week from the first to the last day of radiation therapy) and adjuvant (150–200 mg per square meter for 5 days during each 28-day cycle) temozolomide, according to the protocol reported by Stupp et al.<sup>3</sup> Nevertheless, due to the large timeframe evaluated in the study, we included patients treated with different protocols. Before concomitant and adjuvant chemoradiotherapy with temozolomide had become the standard treatment for newly diagnosed malignant astrocytoma,<sup>3</sup> patients were treated with nitrosourea-based chemotherapy administered concurrently with radiation therapy. If tumor recurrence or progression was documented, we considered salvage surgery, additional radiation therapy, and/or additional chemotherapy (temozolomide, nitrosoureas, or bevacizumab plus irinotecan). Treatment with steroids was reduced to the minimum needed for clinical control of symptoms.

Patient survival after undergoing <sup>1</sup>H-MRS was studied. For those patients who survived past the date of our analysis (*n* = 27), survival was right censored in the survival analysis to February 15, 2010. In 15 patients, we could determine only that the patients were alive on a particular date, and these patients were lost to follow-up. They were right censored in the analysis to the known time interval. The main body of the study was made up of the patients for whom the date of

**Table 1: Patient data and prognostic factors in 145 noncensored patients with HGA**

Prognostic Factor	No.	Survival (median) (95% CI)
Age <sup>a</sup>		
<50 years	21	330 (34–975)
≥50 years	124	178 (39–927)
Sex		
Men	89	175 (41–924)
Women	56	201 (40–954)
WHO grade <sup>b</sup>		
Anaplastic astrocytoma (III)	27	254 (43–963)
Glioblastoma (IV)	118	178 (39–937)
Karnofsky Performance Status <sup>a</sup>		
<70	46	108 (39–472)
70–80	56	197 (59–887)
>80	43	278 (57–1238)
Extent of surgery <sup>b</sup>		
Biopsy	56	137 (28–849)
Partial resection	53	197 (54–839)
Complete resection	36	363 (63–1265)
Treatment <sup>b</sup>		
Conservative support	55	92 (28–249)
Radiotherapy	27	222 (94–461)
Chemoradiotherapy	63	330 (109–1154)

<sup>a</sup> No significant differences were found when only the noncensored patients were evaluated, but the differences reached significance level when the censored patients were included in the survival analysis.

<sup>b</sup> Significant differences were found with the logrank test.

death was known (total, 145 patients who provided 140 spectra at STE and 140 spectra at LTE). These cases were used for all the computations, while right-censored cases were only included for the survival analysis with the Kaplan method and Cox proportional hazards model.

### <sup>1</sup>H-MRS

Single-voxel <sup>1</sup>H-MRS was performed with a 1.5T MR imaging unit (Philips Healthcare, Best, the Netherlands) as the last sequence of the MR imaging examination. A VOI between 1.5 and 2 cm<sup>3</sup> was placed following criteria previously approved at our institution for performing <sup>1</sup>H-MRS in brain tumors. Specifically, the VOI size and location were determined with the aim of positioning the largest possible voxel within the solid brain mass, with minimal contamination from the surrounding nonaffected tissue or from nonenhancing areas of the tumor, when possible. Two spectra were acquired from the same VOI: 1) SE STE (TR/TE/averages, 2000/30/96–192) and 2) SE LTE (TR/TE/averages, 2000/136/128–256). Spectrum analysis was performed offline with the use of the jMRUI software (<http://sermn02.uab.cat/mrui>).<sup>18</sup> All spectra were consecutively processed by the same spectroscopist (C.M.), who has 12 years of experience in spectroscopy and who was blinded to patient data in the processing sessions. Zero-order phase of the spectra was manually corrected when appropriate. Chemical shifts in the frequency domain were internally referenced to the peaks of creatine at 3.03 ppm or choline compounds at 3.21 ppm. Each free induction decay was Fourier-transformed with 1-Hz line-broadening. The intensities of the points of the spectrum included between 0.00 and 4.00 ppm (*I*<sub>0.00</sub>–*I*<sub>4.00</sub>; total, 131 points) were selected and used as input for the normalization and statistical analysis. The data vector was normalized to unit-length.<sup>19,20</sup> With this method, the squares of the intensities of each point were summed and the normalized intensity values (*NI*<sub>xxx</sub>) were obtained by dividing the intensity value of each point by the square root of this sum:

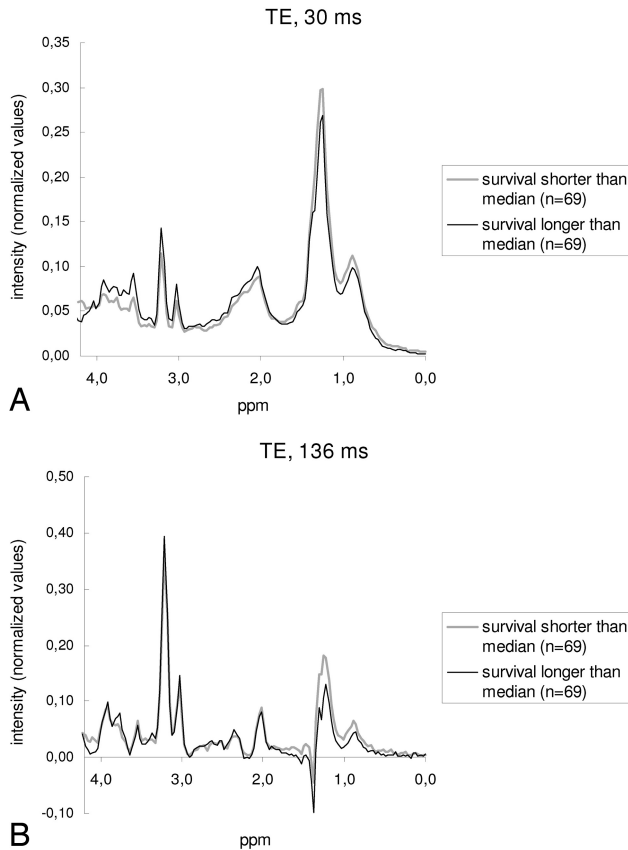


**Fig 1.** Average spectra obtained with the dataset of noncensored patients dichotomized into 2 subgroups depending on survival better or worse than the median value (187 days). A, STE spectra. The main differences are seen in the mobile lipid region (all around 0.90 and 1.30 ppm) and in the region between 3.40 and 3.90 ppm. Two representative spectroscopy points were defined in the statistical analysis in the positions 0.98 and 3.67 ppm. B, LTE spectra. Significant differences are found in the mobile lipid region at this TE. Two representative spectroscopy points were defined in the positions 0.98 and 1.25 ppm.

$$(NI_{x,xx} = I_{x,xx} / [\sum_{n=0.00-4.00} I_n^2]^{1/2}).$$

## Statistics

From the statistical point of view, the spectra were considered a series of numbers that delineate the graphics shown as spectra. We considered each point in the spectrum to be a variable for the statistical

analysis. The first step in the study was to select the variables that could provide a better prognostic assessment. To do this, we dichotomized the datasets of patients for whom the dates of death were known into 2 groups: 1) patients with survival better than the median, and 2) patients with survival worse than the median. Both groups were compared using the Mann-Whitney *U* nonparametric test. We considered that the points of the spectrum that showed the most significant differences in the statistical test were those that could better differentiate the 2 prognostic groups. To improve the consistency of the results, we used only those points having  $\geq 2$  neighboring points with significant differences. This method, which has been previously used,<sup>19</sup> helps to avoid some differences that could occur due to chance. To obtain an easily implementable index for clinical practice, we generated ratios between selected spectroscopy points and evaluated them when possible. We considered that the ideal situation for constructing a ratio with 2 spectroscopy points was that in which the intensities of both points showed an opposing tendency in the prognostic groups (ie, high intensity value of 1 point in the poor prognosis group and low intensity value of the other point). Accordingly, ratios were constructed only when 2 of the spectroscopy points selected with the Mann-Whitney *U* test showed an opposing tendency in relation to survival.

The previous step of the statistical analysis was used as feature selection, and only the selected spectroscopy points and ratios were used for further analysis of survival. We constructed a method to stratify patients into 2 groups hypothesized to represent patients with good and poor prognosis. For this method, threshold values for the selected variables were obtained by constructing ROC curves. The groups generated were compared using the Kaplan-Meier method to detect differences in survival by means of logrank statistics. Survival modeling was performed in 3 patient populations: the population of all patients, a subgroup of patients treated with chemoradiotherapy, and a subgroup of patients who received only conservative support treatment, because we wanted to evaluate the applicability of the predictive potential of spectroscopy for each group. The Cox proportional hazards model with forward stepwise model selection analysis was used to determine which variables had a stronger potential for predicting survival in HGA and, accordingly, could be considered the best-suited for a prognostic assessment. This method includes the variables in the modeling of survival in a stepwise model. In the first step, the method chooses the variable that provides the strongest pre-

**Table 2: Representative spectroscopy points and prognostic performance**

Overall Patients					Patients Treated with Chemoradiotherapy			Conservative-Support Treatment		
Variable	Value	No.	Hazard Ratio (95% CI)	P	No.	Hazard Ratio (95% CI)	P	No.	Hazard Ratio (95% CI)	P
STE <sup>a</sup>										
NI <sub>0.98</sub>	<0.1024	133	0.568 (0.391–0.826)	.003	72	0.424 (0.231–0.778)	.006	38	0.575 (0.323–1.026)	NS
	>0.1024	47	1.000		18	1.000		20	1.000	
NI <sub>3.67</sub>	<0.0473	71	1.992 (1.421–2.792)	<.001	29	2.080 (1.238–3.495)	.006	28	2.038 (1.122–3.699)	.018
	>0.0473	109	1.000		61	1.000		30	1.000	
STE <sup>b</sup>										
I <sub>3.67</sub> /I <sub>0.98</sub>	<0.5510	76	1.866 (1.329–2.621)	<.001	34	2.673 (1.582–4.517)	<.001	29	1.960 (1.071–3.586)	.029
	>0.5510	104	1.000		56	1.000		29	1.000	
LTE <sup>a</sup>										
NI <sub>0.98</sub>	<0.0267	103	0.426 (0.304–0.597)	<.001	57	0.417 (0.249–0.698)	.001	38	0.472 (0.259–0.860)	.014
	>0.0267	79	1.000		32	1.000		21	1.000	
NI <sub>1.25</sub>	<0.0098	59	0.400 (0.272–0.590)	<.001	39	0.434 (0.252–0.748)	.003	10	0.412 (0.187–0.905)	.027
	>0.0098	123	1.000		50	1.000		49	1.000	

<sup>a</sup> Intensity values of points normalized to unit-length:  $NI_{x,xx}$

<sup>b</sup> Ratio between intensity signals of points:  $I_{x,xx}/I_{y,xx}$

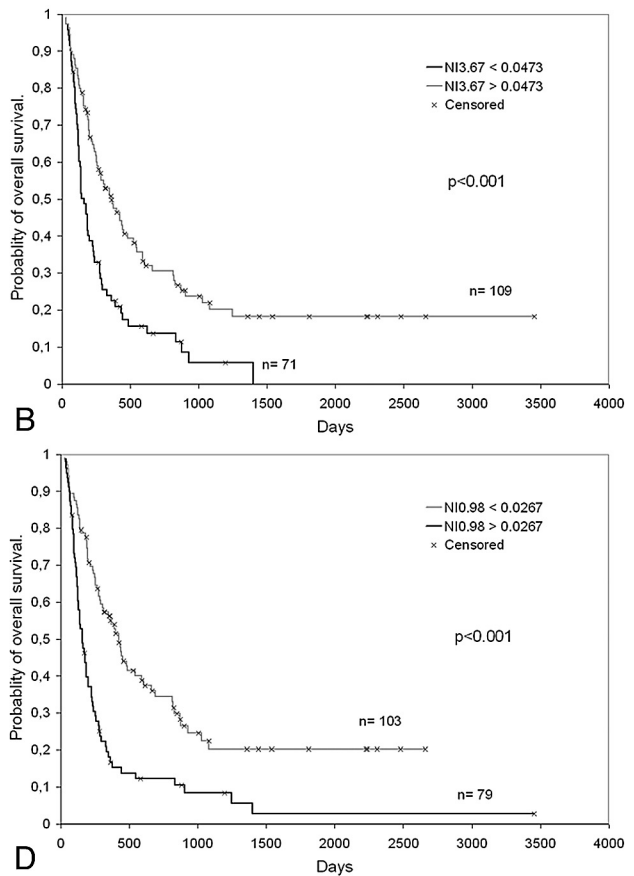
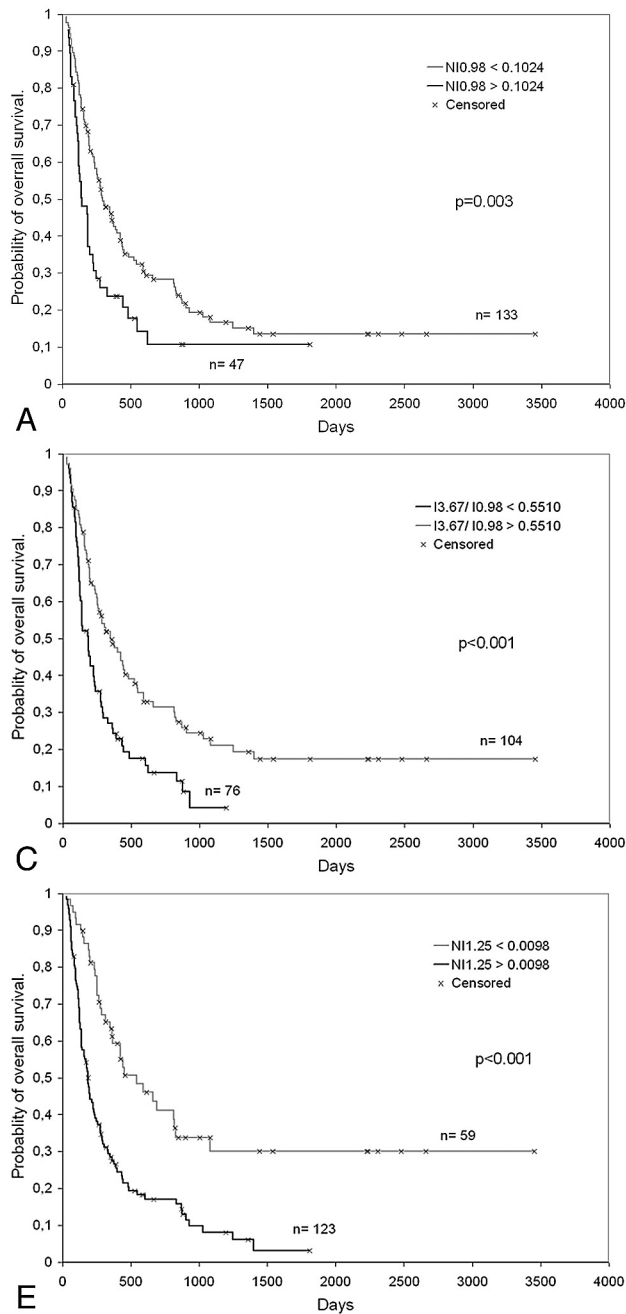


**Fig 2.** Survival curves for patients are dichotomized by the following: the intensity value of the spectroscopy point 0.98 ppm at STE, normalized to unit-length ( $NI_{0.98}$ ) (A), the intensity value of the point 3.67 ppm at STE, normalized to unit-length ( $NI_{3.67}$ ) (B), the value of the ratio between the intensities of the points 3.67 and 0.98 ppm at STE ( $I_{3.67}/I_{0.98}$ ; note that no additional normalization is required for ratios) (C), the intensity value of the point 0.98 ppm at LTE, normalized to unit-length ( $NI_{0.98}$ ) (D), and the intensity value of the point 1.25 ppm at LTE, normalized to unit-length ( $NI_{1.25}$ ) (E).

diction of survival. At each step, the method selects the candidate variable that improves the prediction of survival the most and stops adding variables when adding a new variable will not significantly improve the potential for predicting survival. Prognostic variables evaluated in the model were both clinical (age, sex, WHO grade, KPS, extent of surgery, and treatment administered) and spectroscopic (the normalized intensities of spectroscopy points and the ratios selected in the first step of the analysis). Differences of  $P < .05$  were considered statistically significant.

## Results

A total of 187 patients fulfilled the inclusion criteria and were retained in the study. At the time of last assessment (February 15, 2010), 27 patients were alive after 879 days of median follow-up (range, 266–3454 days). Follow-up for deceased patients ranged between 23 and 1400 days (median, 187 days).

Additionally, 15 patients were lost to follow-up after 315 days of median follow-up (range, 83–1078). Patient data and known prognostic factors are shown in Table 1. The dataset of 145 patients for whom the date of death was known was dichotomized into 2 groups: survival shorter than (71 patients, 69 spectra at STE and 69 at LTE) and longer than (72 patients, 69 spectra at STE and 69 at LTE) the median survival value (187 days). The average spectra for these groups are shown in Fig 1. Two points of the spectrum at STE were selected for further analysis according to the criteria defined in the “Materials and Methods” section, 0.98 ppm ( $P < .001$ ) and 3.67 ppm ( $P = .006$ ), and another 2, at LTE, 0.98 ppm ( $P < .001$ ) and 1.25 ppm ( $P = .011$ ). The ratio between the intensities at points 3.67 and 0.98 ppm was calculated for STE spectra ( $I_{3.67}/I_{0.98}$ ) and was included in the analysis. No representative point with significant differences was found at an LTE that could



**Table 3: Multivariate analysis of prognostic factors using the Cox proportional hazards model with forward stepwise selection in 180 patients with HGA and spectra obtained at STE<sup>a</sup>**

Variable/Value	No.	Hazard Ratio (95% CI)	P
Clinical parameters/treatment			<.001
Conservative support	58	11.564 (7.242–18.465)	
Radiotherapy alone	31	1.768 (1.100–2.841)	
Chemoradiotherapy	91	1.000	
Spectroscopy parameters			
Intensity signals normalized to unit-length (NI)			
NI <sub>3.67</sub>			<.001
<0.0473	71	2.132 (1.504–3.023)	
>0.0473	109	1.000	

<sup>a</sup> Age (<50 years vs >50 years), sex, WHO grade, KPS, extent of surgery, the spectroscopic parameters normalized intensity signal at 0.98 ppm, and the ratio between intensity signals at 3.67 and 0.98 ppm were not selected as elective prognostic factors.

**Table 4: Multivariate analysis of prognostic factors using the Cox proportional hazards model with forward stepwise selection in 182 patients with HGA and spectra obtained at LTE<sup>a</sup>**

Variable/Value	No.	Hazard Ratio	P
Clinical parameters/treatment			<.001
Conservative support	58	12.241 (7.556–19.831)	
Radiotherapy alone	34	1.784 (1.116–2.853)	
Chemoradiotherapy	90	1.000	
Spectroscopy parameters			
Intensity signals normalized to unit-length (NI)			
NI <sub>0.98</sub>			<.001
<0.0267	103	0.499 (0.339–0.736)	
>0.0267	79	1.000	
NI <sub>1.25</sub>			.015
<0.0098	60	0.574 (0.368–0.897)	
>0.0098	122	1.000	

<sup>a</sup> Age (<50 years vs > 50 years), sex, WHO grade, KPS, and extent of surgery were not selected as elective prognostic factors.

be used to construct a ratio with the resonances of 0.98 and 1.25 ppm. Accordingly, ratios were not used for LTE spectrum analysis.

Threshold values for discriminating groups are shown in Table 2, along with their prognostic performance. All the spectroscopy points selected in the feature selection step with the Mann-Whitney *U* test method provided stratification of patients in groups with significant differences in survival, assessed with the Kaplan-Meier method (*P* between <.001 and .003). This was true for all spectroscopy points and subgroups of patients with the exception of NI<sub>0.98</sub> at STE in the conservative-support treatment group, which did not reach statistical significance. Multivariate analysis revealed that the prognostic value of spectroscopic variables was independent of age, sex, WHO histologic grade, extent of surgery, KPS, and treatment administered. Figure 2 shows some survival curves calculated with representative spectroscopy points and ratios.

Two variables were selected in the Cox proportional hazards model with forward stepwise selection in the group of patients studied with STE <sup>1</sup>H-MRS: treatment administered and NI<sub>3.67</sub> (Table 3). Three variables were selected in the group studied with LTE <sup>1</sup>H-MRS: treatment administered, NI<sub>0.98</sub>, and NI<sub>1.25</sub> (Table 4). Figure 3 shows 2 representative examples of the application of our findings.

## Discussion

We found that <sup>1</sup>H-MRS could be used to stratify prognostic groups in HGA and that this prognostic assessment could be made by evaluating the intensity values of 2 points on the spectrum at STE (0.98 and 3.67 ppm) and another 2 at LTE (0.98 and 1.25 ppm).

Recent advances in treatment of gliomas have improved overall survival and progression-free survival,<sup>3,4</sup> but these treatments are not totally safe, and adverse effects can appear in a non-negligible number of patients. Accordingly, it is important to define patients who can take advantage of intensive treatments and those for whom a conservative support treatment is a choice. Histopathology remains the reference standard for prognostic assessment, providing an insight into the morphologic cytostructure of the tumor.<sup>1</sup> Nevertheless, histopathology has its limitations in providing prognostic value, and additional factors have been defined for stratifying patients into diverse prognostic groups. A recursive partitioning analysis undertaken by the Radiation Therapy Oncology Group identified 4 risk classes for glioblastoma based on patient age, KPS, neurologic function, mental status, and extent of surgery.<sup>9,21</sup> These items provide a prognostic assessment based on factors related to patient status and effectiveness of the surgical approach.

A subanalysis by the European Organization for Research and Treatment of Cancer and the National Cancer Institute of Canada included the MGMT promoter methylation status as an independent prognostic factor.<sup>10</sup> Because of the way the evaluation of the MGMT promoter methylation status provides an insight into the ability of the tumor to repair DNA damage, this work introduces a third milestone in the approach to prognosis of malignant astrocytomas. In addition to tumor cytostructure and patient performance status, the functionalism and the metabolomic profile of tumor cells could add useful information for specifying the prognosis of a particular case. Our study has shown that the information provided by <sup>1</sup>H-MRS may be of help in the prognostic assessment of patients. Selection of spectroscopic variables with the Cox stepwise forward model should be taken as strong support for the prognosis value of <sup>1</sup>H-MRS in HGA. We consider that these findings, though promising, should be confirmed in a prospective study. Nevertheless, they suggest that there might be some metabolic information in tumors that could help in specifying the prognosis of HGA and that this information could be assessed in a noninvasive way by <sup>1</sup>H-MRS.

<sup>1</sup>H-MRS is an MR imaging technique that provides biochemical information about the tissue being studied. In the field of brain tumors, this information has proved useful for discriminating tumors and pseudotumoral lesions,<sup>22,23</sup> for discriminating between tumor types,<sup>19</sup> and for assessing the WHO grade of glial tumors.<sup>24</sup> In the present study, we found several regions of the spectrum that have prognostic value. The regions corresponding to 0.98 and 1.25 ppm have been attributed to the methyl and methylene groups of mobile lipids and have been correlated with tumoral necrosis.<sup>25</sup> Lactate could also make some contribution to the resonance at 1.25 ppm. Our study demonstrates that there is an inverse correlation between resonance intensity in these regions at both STE and LTE and patient survival (a high-intensity value of the peaks at 0.98 and 1.25 ppm correlates with low survival). More

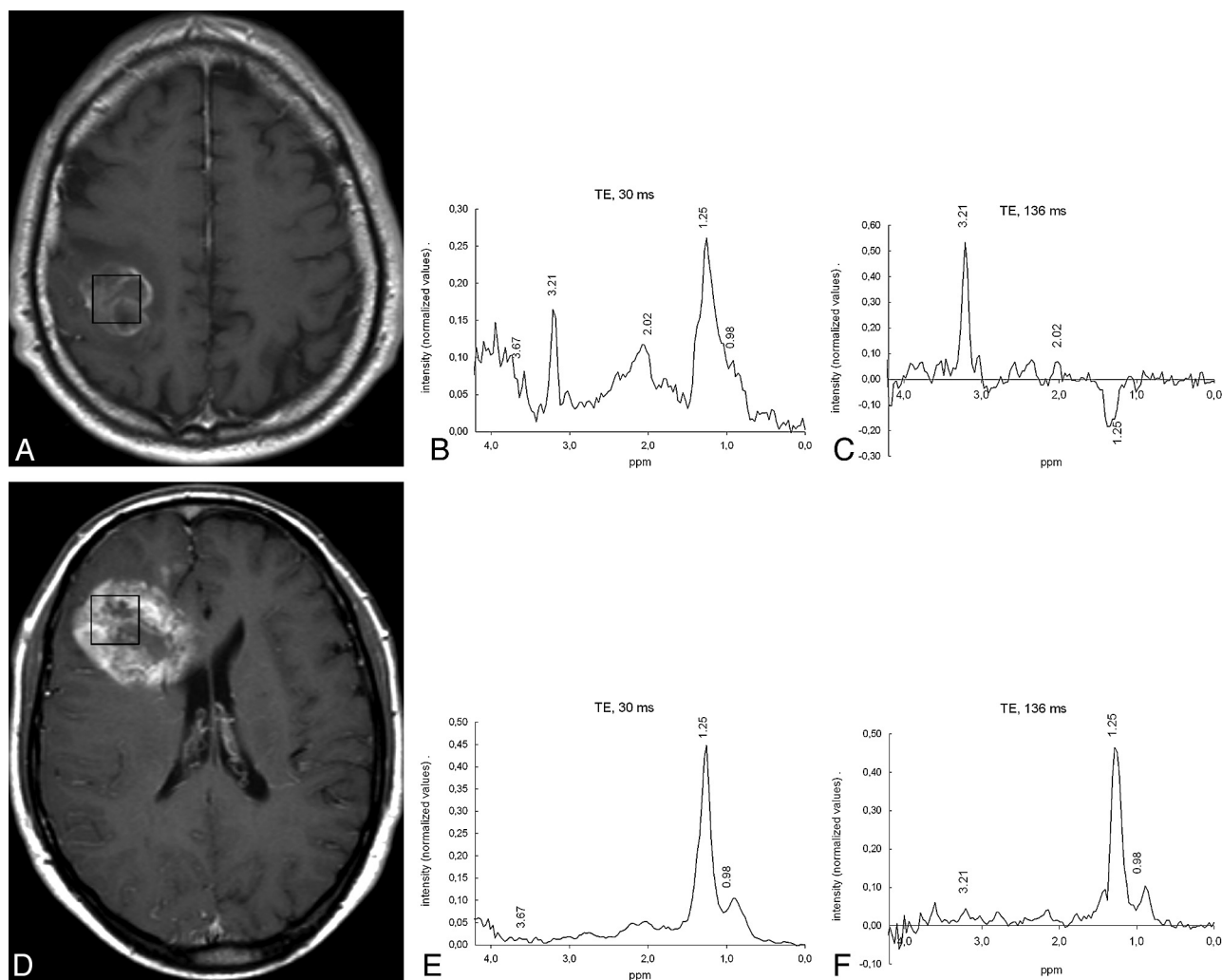


**Fig 3.** Representative cases of the prognostic value of  $^1\text{H}$ -MRS. *A*, Axial T1-weighted postcontrast image in a 53-year-old man shows a right frontoparietal necrotic mass. The box shows the VOI used for spectroscopy. The patient's KPS score after surgical debulking was 80. Treatment with chemoradiotherapy was performed. *B*, STE spectrum shows the presence of lipids at both 0.90 and 1.30 ppm, a large Cho peak (centered at 3.21 ppm), and various resonances between 3.55 and 4.00 ppm. The elective spectroscopy parameter at this TE was in the range of patients with long survival ( $\text{NI}_{3.67} = 0.0623$  [ $>0.0473$ , good prognosis]) as well as the value of the ratio (ratio  $I_{3.67}/I_{0.98} = 0.7425$  [ $>0.5510$ , good prognosis]). *C*, LTE spectrum shows no signals of mobile lipids at this TE. The elective spectroscopy parameters at this TE were also in the range of patients with long survival ( $\text{NI}_{0.98} = -0.0316$  [ $<0.0267$ , good prognosis],  $\text{NI}_{1.25} = -0.1087$  [ $<0.0098$ , good prognosis]). The patient was alive at the end of the study, after 1004 days of follow-up. *D*, Axial T1-weighted image in a 59-year-old man shows a right frontal necrotic mass. The patient's KPS score after surgical debulking was 70. Treatment with chemoradiotherapy was performed. *E*, The STE spectrum shows prominent lipid peaks with little contribution of other resonances. The elective spectroscopy parameter and the ratio suggest poor prognosis ( $\text{NI}_{3.67} = 0.0097$  [ $<0.0473$ , poor prognosis], and ratio  $I_{3.67}/I_{0.98} = 0.1124$  [ $<0.5510$ , poor prognosis]). *F*, The LTE spectrum also shows a clear dominance of lipid peaks. The elective spectroscopy parameters at this TE were also in the poor prognosis range ( $\text{NI}_{0.98} = 0.0452$  [ $>0.0267$ , poor prognosis],  $\text{NI}_{1.25} = 0.4452$  [ $>0.0098$ , poor prognosis]). The patient died after 110 days of follow-up.

interesting is the finding that another region of the STE spectrum, around 3.67 ppm, showed a direct correlation with patient survival (a high-intensity value of the peak at 3.67 ppm correlates with high survival). Prior studies showed some prognostic value of the major resonances of the spectrum, such as choline-containing compounds, *N*-acetylaspartate, creatine, lipids, and lactate.<sup>16,17</sup> The methodology used in our study provided the opportunity to detect differences in the area around 3.67 ppm, not evaluated in previous studies. This spectroscopy point offers the opportunity to formulate a ratio between metabolites at STE to be used in a clinical setting. Using ratios would have the advantage of producing a straightforward quantitative assessment of the spectrum that would not require any additional normalization procedure. Accordingly, STE  $^1\text{H}$ -MRS may be considered somewhat superior to LTE  $^1\text{H}$ -MRS for prognostic assessment of HGA in a real clin-

ical situation. Nevertheless, spectra at both TEs may provide relevant information.

Three spectroscopic variables and the clinical parameter "treatment administered" were selected in the multivariate analysis. We consider that these variables should be viewed as the ones with the greatest prognostic significance. Accordingly, finding a  $\text{NI}_{3.67} > 0.0473$  at STE, an  $\text{NI}_{0.98} < 0.0267$  at LTE, and/or an  $\text{NI}_{1.25} < 0.0098$  at LTE would correlate with good prognosis (Tables 3 and 4). It was not possible in this study to define precisely which metabolite or metabolites could explain the prognostic value of spectroscopy found in the area around 3.67 ppm. Nevertheless, because of the extent of the region involved in the mean spectra (Fig 1), the fact that it was only identifiable at STE,<sup>26</sup> and the similarity between the spectral pattern of the region and that of glucose in a phantom,<sup>27</sup> we hypothesize that glucose can play a role in this. A

possible explanation for our findings is that high metabolic activity and consequently poor prognosis correlate with depletion of glucose in the extracellular compartment and, accordingly, with low intensity of the resonances that represent this compound in the spectra, centered at 3.67 ppm. Other compounds, such as glutamine, glutamate, glycerophosphocholine,<sup>28</sup> macromolecules, and lipid metabolites, may also play a role. Further ex vivo and in vitro examination is needed for a more precise assessment of the metabolites involved in these differences.<sup>29</sup>

Our analysis has several possible limitations. One consideration is patient selection. Fifty of 270 eligible spectra at STE (19%) and 48 at LTE (18%) were excluded because of poor-quality data. This exclusion limits the usefulness of <sup>1</sup>H-MRS in a clinical context. Nevertheless, we did perform <sup>1</sup>H-MRS as the last sequence of the MR imaging study. In view of our results, spectra of poor quality should be repeated in a specific spectroscopic examination when necessary, and then the rate of patients excluded would, hopefully, be significantly reduced. Another limitation is related to the retrospective nature of the study. We consider that this study provides the first evidence of the prognostic and predictive value of <sup>1</sup>H-MRS in HGA. Nevertheless, future prospective work should improve and validate the application of <sup>1</sup>H-MRS in clinical practice by suggesting partitioning and including <sup>1</sup>H-MRS in the scores. A final concern is the technique for performing spectroscopy. Parameters such as voxel size and positioning are difficult to standardize, and this difficulty results in a certain amount of variability. A consequence of this variability is that it might be necessary to recalculate thresholds for classification at each center to obtain optimal results.

## Conclusions

In our study, we analyzed the whole range of the MR spectra obtained in patients with HGA, to define which regions were the most relevant for a prognostic assessment. We found that 2 points at STE, 0.98 and 3.67 ppm, and another 2 at LTE, 0.98 and 1.25 ppm, provided relevant prognostic information. These points were selected as prognostic factors in a stepwise multivariate analysis, and their prognostic significance remained even when oncologic treatment was administered. This predictive value of <sup>1</sup>H-MRS concerning survival could be very useful for evaluating whether intensive oncologic therapy is indicated in a particular patient.

## Acknowledgments

We thank Xavier Pérez (Clinical Research Unit of the Institut Català d'Oncologia) for technical advice on statistical data processing.

## References

- Louis DN, Ohgaki H, Wiestler OD, et al. *The 2007 WHO Classification of Tumors of the Central Nervous System*. Lyon, France: IARC Press; 2007
- CBTRUS, The Central Brain Tumor Registry of the United States. **2008 Statistical Report: Primary Brain Tumors in the United States, 1998–2002**. <http://www.cbtrus.org/reports/2007–2008/2007report.pdf>. Accessed July 7, 2009
- Stupp R, Mason WP, van den Bent MJ, et al. **Radiotherapy plus concomitant and adjuvant temozolomide for glioblastoma**. *N Engl J Med* 2005;352:987–96
- Vredenburg JJ, Desjardins A, Herndon JE II, et al. **Phase II trial of bevacizumab and irinotecan in recurrent malignant glioma**. *Clin Cancer Res* 2007;13:1253–59
- Jackson RJ, Fuller GN, Abi-Said D, et al. **Limitations of stereotactic biopsy in the initial management of gliomas**. *Neuro Oncol* 2001;3:193–200
- Prayson RA, Agamanolis DP, Cohen ML, et al. **Interobserver reproducibility among neuropathologists and surgical pathologists in fibrillary astrocytoma grading**. *J Neurol Sci* 2000;175:33–39
- Kros JM, Gorlia T, Kouwenhoven MC, et al. **Panel review of anaplastic oligodendroglioma from European Organization for Research and Treatment of Cancer Trial 26951: assessment of consensus in diagnosis, influence of 1p/19q loss, and correlations with outcome**. *J Neuropathol Exp Neurol* 2007;66:545–51
- Cairncross JG, Ueki K, Zlatescu MC, et al. **Specific genetic predictors of chemotherapeutic response and survival in patients with anaplastic oligodendrogliomas**. *J Natl Cancer Inst* 1998;90:1473–79
- Curran WJ, Scott CB, Horton J, et al. **Recursive partitioning analysis of prognostic factors in three Radiation Therapy Oncology Group malignant glioma trials**. *J Natl Cancer Inst* 1993;85:704–10
- Gorlia T, van den Bent MJ, Hegi ME, et al. **Nomograms for predicting survival of patients with newly diagnosed glioblastoma: prognostic factor analysis of EORTC and NCIC trial 26981–22981/CE. 3**. *Lancet Oncol* 2008;9:29–38. Epub 2007 Dec 21
- Wen PY, Kesari S. **Malignant gliomas in adults**. *N Eng J Med* 2008;359:492–507
- Murakami R, Sugahara T, Nakamura H, et al. **Malignant supratentorial astrocytoma treated with postoperative radiation therapy: prognostic value of pretreatment quantitative diffusion-weighted MR imaging**. *Radiology* 2007;243:493–99
- Pope WB, Kim HJ, Huo J, et al. **Recurrent glioblastoma multiforme: ADC histogram analysis predicts response to bevacizumab treatment**. *Radiology* 2009;252:182–89
- Law M, Young RJ, Babb JS, et al. **Gliomas: predicting time to progression or survival with cerebral blood volume measurements at dynamic susceptibility-weighted contrast-enhanced perfusion MR imaging**. *Radiology* 2008;247:490–98
- Oh J, Henry RG, Pirzkall A, et al. **Survival analysis in patients with glioblastoma multiforme: predictive value of choline-to-N-acetylaspartate index, apparent diffusion coefficient, and relative cerebral blood volume**. *J Magn Reson Imaging* 2004;19:546–54
- Kuztnesov YE, Caramanos MA, Antel SB, et al. **Proton magnetic resonance spectroscopic imaging can predict length of survival in patients with supratentorial gliomas**. *Neurosurgery* 2003;53:565–76
- Li X, Jin H, Lu Y, et al. **Identification of MRI and 1H MRSI parameters that may predict survival for patients with malignant gliomas**. *NMR Biomed* 2004;17:10–20
- van den Boogaart A. **Quantitative data analysis of in vivo MRS data sets**. *Magn Reson Chem* 1997;35:S146–52
- Tate AR, Underwood J, Acosta D, et al. **Development of a decision support system for diagnosis and grading of brain tumours using in vivo magnetic resonance single voxel spectra**. *NMR Biomed* 2006;19:411–34
- Tate AR, Griffiths JR, Martínez-Pérez I, et al. **Towards a method for automated classification of 1H MRS spectra from brain tumours**. *NMR Biomed* 1998;11:177–91
- Scott CB, Scarantino C, Urtasun R, et al. **Validation and predictive power of Radiation Therapy Oncology Group (RTOG) recursive partitioning analysis classes for malignant glioma patients: a report using RTOG 90–06**. *Int J Radiat Oncol Biol Phys* 1998;40:51–55
- Majós C, Aguilera C, Alonso J, et al. **Proton MR spectroscopy improves discrimination between tumor and pseudotumoral lesion in solid brain masses**. *AJNR Am J Neuroradiol* 2009;30:544–51
- Kim SH, Chang KH, Song IC, et al. **Brain abscess and brain tumor: discrimination with in vivo H-1 MR spectroscopy**. *Radiology* 1997;204:239–45
- Negendank WG, Sauter R, Brown TR, et al. **Proton magnetic resonance spectroscopy in patients with glial tumors: a multicenter study**. *J Neurosurg* 1996;84:449–58
- Castillo M, Kwok L. **Proton MR spectroscopy of common brain tumors**. *Neuroimaging Clin North Am* 1998;8:733–52
- Bruhn H, Michaelis T, Merboldt KD, et al. **Monitoring cerebral glucose in diabetics by proton MRS**. *Lancet* 1991;337:745–46
- Moreno-Torres A, Martínez-Pérez I, Baquero M, et al. **Taurine detection by proton magnetic resonance spectroscopy in medulloblastoma: contribution to noninvasive differential diagnosis with cerebellar astrocytoma**. *Neurosurgery* 2004;55:824–29
- Righi V, Roda JM, Paz J, et al. **1H HR-MAS and genomic analysis of human tumor biopsies discriminate between high and low grade astrocytomas**. *NMR Biomed* 2009;22:629–37
- Grand S, Passaro G, Ziegler A, et al. **Necrotic tumor versus brain abscess: importance of amino acids detected at 1H MR spectroscopy-initial results**. *Radiology* 1999;213:785–93